Diamond & Related Materials 139 (2023) 110370

Contents lists available at ScienceDirect

Diamond & Related Materials

journal homepage: www.elsevier.com/locate/diamond

DFT study of SCN^- adsorption effect on structural and electronic properties of $Si_{12}C_{12}$ fullerenes

Fangyuan Li [a,*], Fay Fathdal [b], Gufran Abd [c], Jameel Mohammed Ameen Sulaiman [d], Safaa Mustafa Hameed [e], Sarah Salah Jalal [f], Usama S. Altimari [o], Israa Alhan [g], Ibrahim H. Alkersan [h,i,j], Ali H. Alsalamy [k], Elham Tazikeh-Lemeski [l,*], Andrew Ng Kay Lup [m,n]

[a] Zhejiang Business Technology Institute, Ningbo, Zhejiang 315012, China
[b] College of Medical Techology, Al-Farahidi University, Iraq
[c] Al-Manara College for Medical Sciences, Maysan, Iraq
[d] Department of Dental Industry Techniques, Al-Noor University College, Nineveh, Iraq
[e] Department of Optics, College of Health & Medical Technology, Sawa University, Almuthana, Iraq
[f] College of Pharmacy, National University of Science and Technology, Dhi Qar, Iraq
[g] Engineering Department, Mazaya University College, Dhi Qar, Iraq
[h] College of Technical Engineering, the Islamic University, Najaf, Iraq
[i] College of Technical Engineering, the Islamic University of Al Diwaniyah, Iraq
[j] College of Technical Engineering, the Islamic University of Babylon, Iraq
[k] College of Technical Engineering, Imam Ja'afar Al-Sadiq University, Al-Muthanna 66002, Iraq
[l] Department of Chemistry, Gorgan Branch, Islamic Azad University, Gorgan, Iran
[m] College of Chemistry and Chemical Engineering, Xiamen University, Xiamen 361005, Fujian, China
[n] School of Energy and Chemical Engineering, Xiamen University Malaysia, Jalan Sunsuria, Bandar Sunsuria, 43900 Sepang, Selangor Darul Ehsan, Malaysia
[o] Department of Medical Instruments Engineering Techniques, Al-Nisour University College, Baghdad, Iraq

ARTICLE INFO

Keywords:
$Si_{12}C_{12}$
SCN^-
Adsorption
Electronic properties
Infrared spectrum
DFT

ABSTRACT

Utilizing density functional theory (DFT) calculations, the adsorption characteristics and electronic structure of thiocyanate anion (SCN^-) through nitrogen and sulfur heads upon the $Si_{12}C_{12}$ surface were investigated by the B3LYP functional and 6–31 + G** standard basis set. The results express that the covalent interaction of SCN^- through the nitrogen head (−3.08 eV) is stronger in comparison with the sulfur head of SCN^- (−2.32 eV) to the fullerene surface. Additionally, the interaction of two SCN^- through nitrogen head has weaker surface adsorption on the silicon-carbon (Si—C) atom (−1.27 eV) in comparison with the Si—Si atom (−2.78 eV) of $Si_{12}C_{12}$ fullerene. The influence of SCN^- adsorption on the $Si_{12}C_{12}$ surface was characterized by the infrared (IR) absorption spectrum. A significant orbital hybridization between SCN^- and $Si_{12}C_{12}$ fullerenes occurred during the adsorption process, according to the computed density of states (DOS). According to the analysis of binding energy, energy gap, and dipole moment, $Si_{12}C_{12}$ fullerene can be applied to SCN^- removal applications. Based on the thermodynamic parameters, the negative Gibbs free energy (ΔG) and enthalpy change (ΔH) values confirmed that the SCN^- adsorption by the nitrogen heads on the $Si_{12}C_{12}$ surface was spontaneous and exothermic.

1. Introduction

Silicon carbide (SiC) nanostructures of various dimensions (for instance, the 0-D nanoclusters, 1-D nanotubes, and 2-D ultrathin films) are currently the focus of extensive research because of their special qualities (high hardness, high resistance, excellent thermal conductivity, wide bandgap, and excellent chemical and physical stability) [1]. Moreover, researchers have reported SiC nanostructures as a practical substrate for biomaterial and biosensing applications [2,3]. The chemical, electronic, and magnetic characteristics of nanoclusters have been shown to be significantly influenced by their size and composition [4–6]. Up until now, a lot of research has been done on the advantages of SiC nanostructures for the adsorption of gaseous pollutants, especially when using computational methods [7,8]. For instance, Solimannejad

* Corresponding authors.
E-mail addresses: fangyuan202202@126.com (F. Li), elham_tazike@yahoo.com (E. Tazikeh-Lemeski).

https://doi.org/10.1016/j.diamond.2023.110370
Received 3 March 2023; Received in revised form 21 August 2023; Accepted 3 September 2023
Available online 9 September 2023

and co-authors assessed the cyanogen (NCCN) adsorption on the $Si_{12}C_{12}$ and $Si_{12}CuC_{12}$ nanocages using DFT calculations [9]. They have shown the weak physisorption of the NCCN onto the $Si_{12}C_{12}$ surface. In addition, they found that the structural and electronic characteristics of pure $Si_{12}C_{12}$ did not vary drastically during the adsorption process. Javan used DFT calculations to study the adsorption behavior of CO and NO gases on *zigzag* (10,0) SiCNT and *armchair* (6,6) SiCNT nanotubes and $Si_{12}C_{12}$ nanocages under various conditions [10]. Their findings suggest that both forms of nanotubes can adsorb a CO molecule through chemisorption and physisorption, since their binding energies are around 0.95 and 0.89 eV in the most stable configuration. The adsorption of NO molecule over SiC nanotubes and nanocages was slightly better than the adsorption of CO in its most stable configuration. Alshahrani and co-authors studied $SCN^-@C_{60}$ fullerenes and found that the SCN^- adsorption via its nitrogen head upon the fullerene surface was electrostatic, leading to improvements in the electronic sensitivity of fullerenes to the SCN^- [11]. Baei and co-authors studied the thiocyanate anion (SCN^-) adsorption on the outer wall of single-walled boron nitride nanotubes (SWBNNTs) by DFT calculations [12]. They have found that the boron nitride nanotubes can serve as a new adsorbent to remove SCN^- anion. Earlier studies illustrated the adsorption of SCN^- upon the carbon, boron nitride, boron phosphide, aluminum nitride, and aluminum phosphide nanotubes [13–15]. Recently, the adsorption behavior of hydrazine (N_2H_4) by $Si_{12}C_{12}$ nanocages and the detection performance of $Si_{12}C_{12}$ nanocages for this molecule were reported by Rahimi and Solimannejad [16]. The aim of the present study is to investigate the adsorption behavior and electronic structure of SCN^- interacting with the outer surface of pure SiC fullerenes to gain further insight into the development of new adsorbents for the removal and detection of toxic molecules.

2. Computational details

Using the Gaussian 09 [17], GaussSum [18], and GaussView 5.0.8 suite of programs [19], the analyses of geometric analysis, Mulliken population analysis (MPA), and density of states (DOS) were calculated for each system under consideration. Geometry optimization was carried out using the 6–31 + G** basis set at the B3LYP level [20,21]. The following equation was used to calculate the adsorption energies (E_{ad}) of SCN^- on the $Si_{12}C_{12}$ surfaces.

$$E_{ad} = E_{Si12C12-SCN} - (E_{Si12C12} + E_{SCN^-}) \quad (1)$$

where $E_{(Si12C12\text{-}SCN)}$, $E_{Si12C12}$, and E_{SCN}, respectively, are the total energies of adsorption complexes, pure $Si_{12}C_{12}$, and isolated SCN^-. Physicochemical properties of SCN^-, SCN^- interacting $Si_{12}C_{12}$ fullerenes were calculated based on the following quantum molecular descriptors (QMD):

$$\mu = -\frac{1}{2}(I + A) \quad (2)$$

$$\chi = -\mu \quad (3)$$

$$\eta = \frac{1}{2}(I - A) \quad (4)$$

$$S = \frac{1}{2\eta} \quad (5)$$

$$\omega = \frac{\mu^2}{2\eta} \quad (6)$$

where μ, I, A, χ, η, S, and ω values are chemical potential, ionization potential, electron affinity, electronegativity, global hardness, global softness, and electrophilicity index, respectively [22–24]. The I and A values were in order defined as negative orbital energies of the highest occupied molecular orbital (HOMO), $-E_{HOMO}$, and the lowest unoccupied molecular orbital (LUMO), $-E_{LUMO}$, based on Koopmans' approximation.

3. Result and discussion

3.1. Adsorption behavior of SCN^- on the $Si_{12}C_{12}$ fullerenes

At the B3LYP/6–31 + G** level of theory, the relaxed geometries of $Si_{12}C_{12}$ and SCN^- are calculated. $Si_{12}C_{12}$ consists of 8 hexagonal and 6 tetragonal rings with Th symmetry and sp^2 hybridization. In pure $Si_{12}C_{12}$, there are two distinct types of Si—C bonds: one with a bond length of 1.835 is shared by a hexagonal and a tetragonal ring (bond 6–4), and the other with a bond length of 1.777 is shared by two hexagonal rings (bond 6–6), according to the most recent computational analysis (Fig. 1). This result is consistent with research conducted in the past by Solimannejad and colleagues [25]. The IR spectrum of $Si_{12}C_{12}$ demonstrates major absorption peaks at approximately 334, 404, 595, 750, 766, 999, and 1042 cm^{-1} due to the Si—C band [26]. The IR spectrum of SCN^- shows the main absorption peaks at stretching modes v_1 (SC, ~739 cm^{-1}) and v_3 (CN, ~2161 cm^{-1}), and a doubly degenerate deformation v_2 (SCN^-, ~484 cm^{-1}). Fig. 1 also displays the lengths of the C≡N and C—S bonds in linear SCN^- molecules and exhibits C2 point group symmetry. This diagram represents that the bond lengths between C≡N, as well as C—S, are approximately 1.823 and 1.672 Å, respectively.

During the adsorption process, when SCN^- through N-head closed to the Si atom of $Si_{12}C_{12}$, the bond lengths between Si_1-C_1 and Si_1-C_2 were increased to 1.895 and 1.841 Å, while when SCN^- through S-head closed to Si atom the bond lengths were increased to 1.890 and 1.839 Å, respectively (see Fig. 2). These bond length changes occurred during the adsorption process, resulting in strong bonding between the nitrogen atom of the SCN^- and the substrate surface. After the adsorption process, the C—S and C≡N bond lengths of SCN^- were altered to 1.187 and 1.605 Å in model I and 1.169 and 1.699 Å in model II, respectively. Khalaji and colleagues [27] experimentally showed that the C—S and C≡N bond lengths of SCN^- are 1.642 and 1.162 Å, respectively. These experimental results are in good agreement with our results. In addition, the adsorption energy of SCN^- obtained from the N-side atoms is larger than that of the S-side atoms.

In the most stable state, for SCN^- adsorption through N-side on Si atom of the pure $Si_{12}C_{12}$, the two species are separated by 1.765 Å and has an E_{bin} of −3.09 e V. These results suggest that the E_{bin} can be viewed as the covalent interaction. Electron localization function (ELF) plots (model I) of $Si_{12}C_{12}$ and SCN^- interacting with $Si_{12}C_{12}$ are calculated BY the Multiwfn software package [28] as shown in Fig. 3. This image reflects the presence of a new covalent bond between the silicon atom (blue) of the fullerene and the oxygen atom (red) of the molecule [29]. Similar to this, the SCN^- adsorption in the most stable configuration (N-side on C atom of the pure $Si_{12}C_{12}$) has an E_{bin} of −0.410 eV and a distance of 1.393 Å, suggesting a weak bonding during adsorption process owing to the electrostatic interaction. Recently, Alshahrani and co-authors demonstrated the interaction of SCN^- through the N-side on the perfect C_{60} with an energy of −0.49 eV and an interaction distance is 1.479 Å [30]. When SCN^- through S-side adsorbed on Si atom of $Si_{12}C_{12}$ fullerene, the estimated distance between the two species is 2.245 Å and an E_{bin} of −2.32 e V (Fig. 4).

After adsorbing SCN^- onto the fullerene surface from the S side, the length of C—N and C—S bonds changed to 1.169 Å and 1.699 Å, respectively. The significant charges of about 0.523 |e| and 0.115 |e| are transferred from $Si_{12}C_{12}$ fullerene to the SCN^- through the N-side and S-side based on the results of MPA analysis. Furthermore, it is obvious that SCN^- computed binding energy over the surface of the $Si_{12}C_{12}$ fullerene is more considerable than those on C_{60} and BNNT surfaces [11,12]. Furthermore, it is obvious that the determined binding energy of SCN^- upon the surface of the $Si_{12}C_{12}$ fullerene is more significant than that of CNT, BNNT, and AlNNT surfaces [12,13,31]. Fig. 5 in the model I

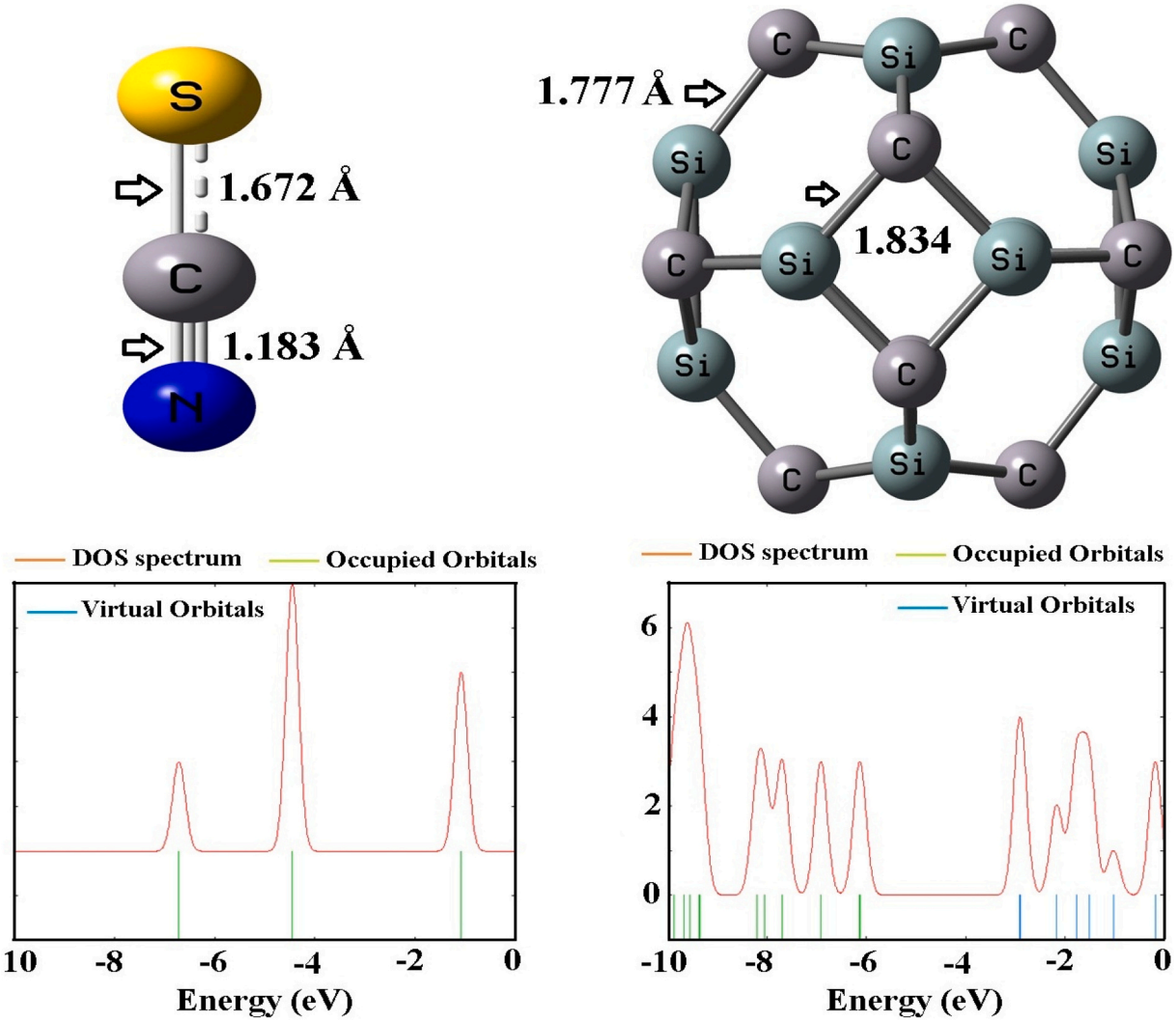

Fig. 1. Optimized structures of $Si_{12}C_{12}$ fullerene and SCN^- molecule.

exhibits theoretical results of three infrared (IR)-active vibrations at 468 cm^{-1}, 980 cm^{-1}, and 2183 cm^{-1} corresponding to ν_1 (SCN^-), ν_2 (SC), and ν_3 (CN), respectively. This suggests that the theoretical results are close to the experimental results mentioned by Lee and co-authors [32]. A sharp peak appearing in the 515 cm^{-1} region is characteristic of ν(Si–NCS) for the model I. The IR absorption peaks of $Si_{12}C_{12}$ fullerene in interaction with the SCN^- changed to 804 and 933 cm^{-1}, while the peaks in the free model appeared at 750, 766, 999, and 1042 cm^{-1}. This result is agreed with obtained results by Karbovnyk and co-authors [33]. Based on the thermodynamic parameters, the changes of ΔG (−2.87 eV) and ΔH (−3.31 eV) confirmed that the SCN^- adsorption by the nitrogen heads on $Si_{12}C_{12}$ surface (model I) was spontaneous and exothermic [34]. For model I, the value of ΔH is more negative compared to the ΔG value, suggesting a decrease in entropy [15,35].

The interaction between the two SCN^- molecules adsorbed on the Si—Si atoms of the $Si_{12}C_{12}$ fullerene is stronger than that of the Si—C atoms of the $Si_{12}C_{12}$ fullerene (Figs. 6–7). The adsorption energies of the two SCN^- molecules on the Si—Si and the Si—C atoms are approximately −2.78 and −1.27 eV respectively. An increase in SCN^- molecules on the Si—C atoms of $Si_{12}C_{12}$ leads to a decrease in the adsorption energy. This result indicates that the Si—Si atoms of $Si_{12}C_{12}$ have a high tendency to adsorb more SCN^- molecules. Soltani et al. reported the adsorption energy of two SCN^-on the B—B atoms of $B_{12}N_{12}$ fullerene is chemisorption (−0.89 eV), a covalent bond is expected to form when each configuration interacts with SCN^- [36]. They also found that the adsorption energy and distance interaction of SCN^- through N-side and S-side on the $B_{11}SiN_{12}$ fullerene in order is −1.61 eV (1.90 Å) and −1.22 eV (2.55 Å). Recently, Alshahrani and co-authors demonstrated the adsorption behavior of SCN^- through the N-side on the pure C_{60} with an energy of −0.49 eV and an interaction distance is 1.479 Å [11]. It is predictable that the size and direction of the dipole moment (μ_D) vector will change as a molecule gets closer to or farther away from a substrate. Examining the results of the μ_D for all configurations, it is hypothesized that the μ_D increased significantly as SCN^- approached different configurations of substrate. Our analysis represent that the μ_D values for pure $Si_{12}C_{12}$ and SCN^- in order are 0.00 and 2.64 Debye (Table 1). The μ_D values of both complexes increased to 18.87 and 17.63 Debye when SCN^- adsorbed to the N-side and S-side positions, respectively, which is comparable with the SCN^- adsorption through N-side on the $B_{12}N_{12}$ (18.25 Debye) and $B_{11}SiN_{12}$ (15.28 Debye) fullerenes [37]. As a result, dipole moment analysis indicates that SCN^- adsorption on $Si_{12}C_{12}$ fullerene caused an increase in polarization and a change in dipole moment [38].

3.2. Molecular orbital (MO) analysis and relative stabilities

Fig. 8 represents frontier molecular orbits (HOMO and LUMO) for a deeper understanding of SCN^- adsorption on the $Si_{12}C_{12}$ surface. The HOMO (E_{HOMO}:−6.13 eV) and LUMO (E_{LUMO}:−2.91 eV) orbitals for $Si_{12}C_{12}$ [39] are distributed around the more electronegative atoms (C)

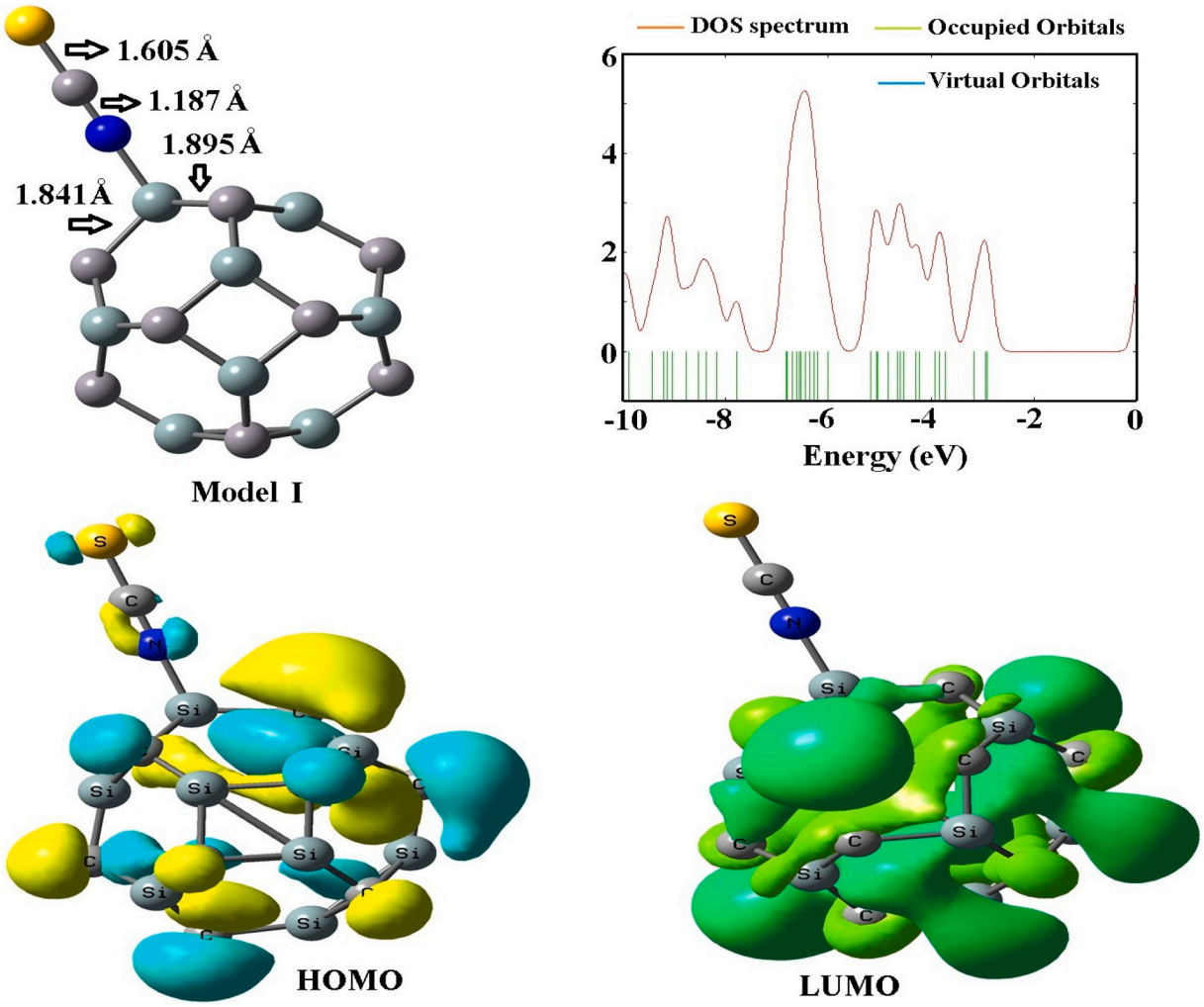

Fig. 2. The optimized structure, FMO, and DOS plots for the $SCN^{-}/Si_{12}C_{12}$ complex.

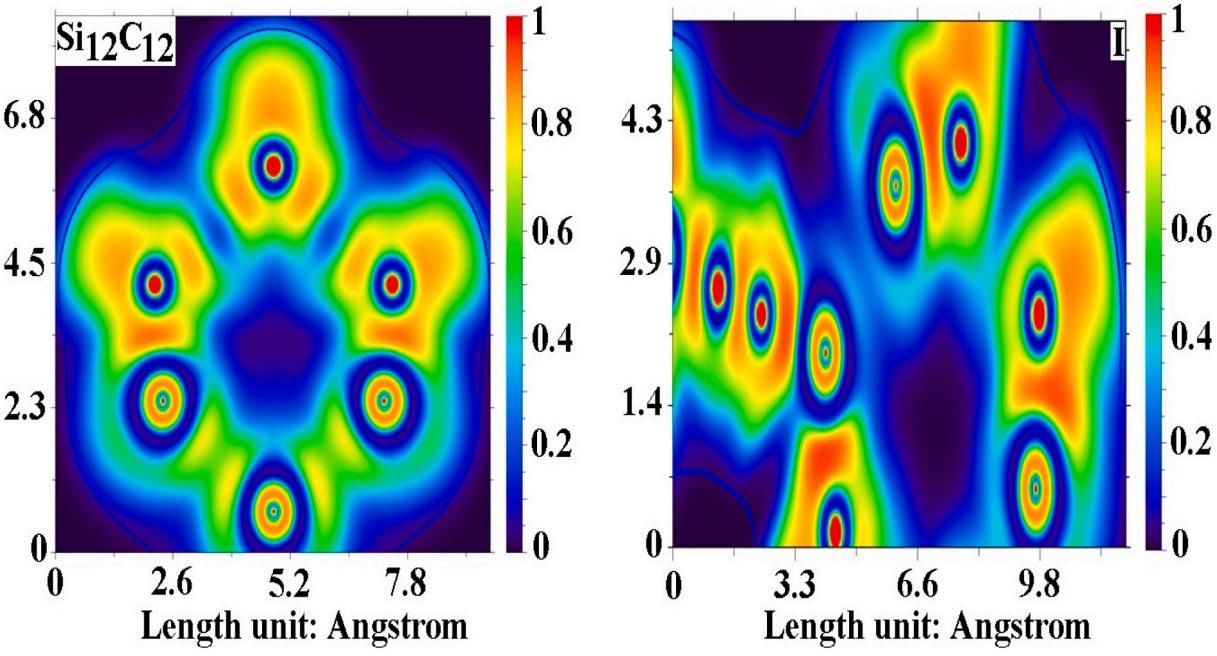

Fig. 3. ELF plots for the $Si_{12}C_{12}$ and $SCN^{-}/Si_{12}C_{12}$ complex (model I).

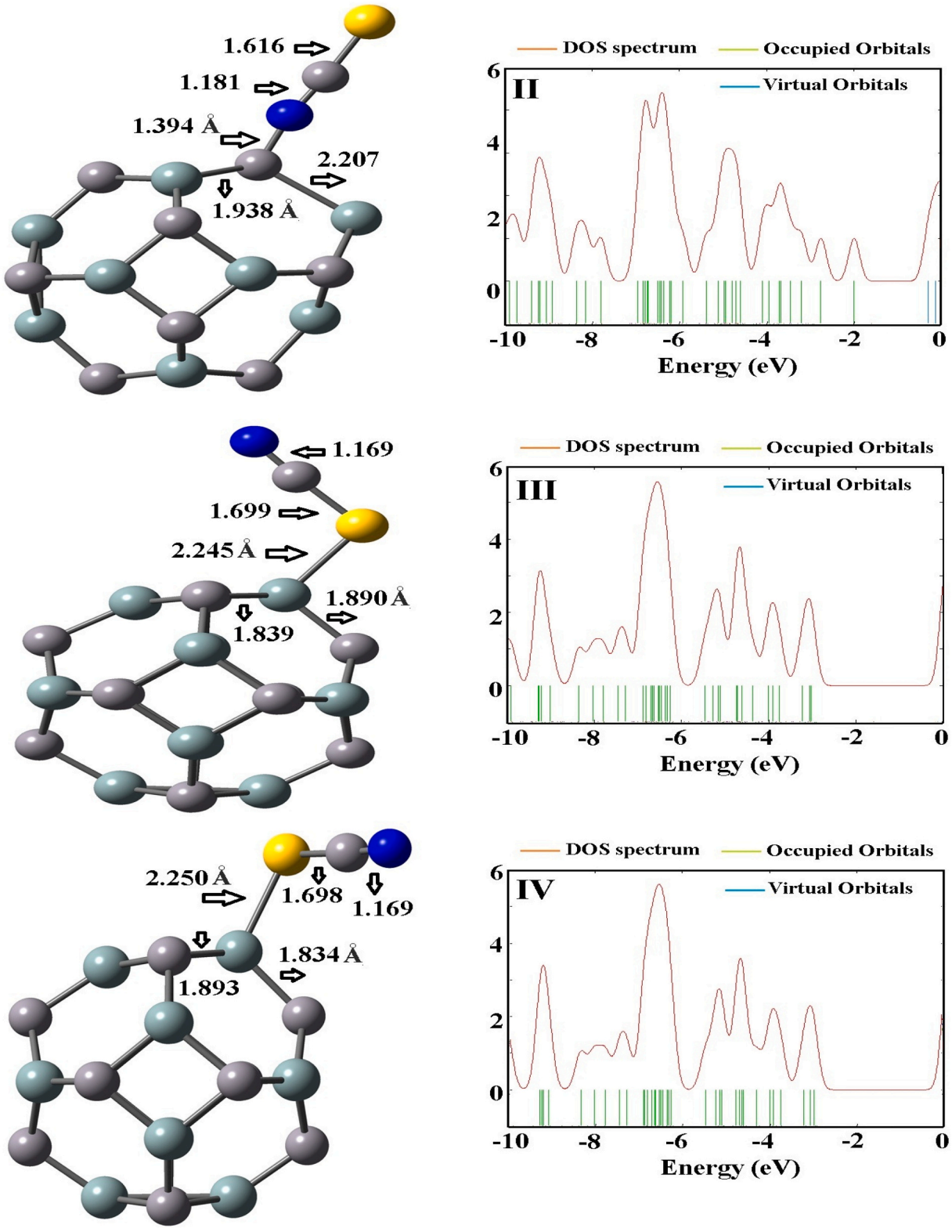

Fig. 4. The optimized geometrics and DOS plots for the different complexes.

and the electropositive atoms (Si), while the HOMO (E_{HOMO}:−1.09 eV) and LUMO (E_{LUMO}: 4.10 eV) orbitals for SCN^- is evenly distributed around the S–C–N bond, as shown in Fig. 8.

The computed energy gap (E_g) values for the pure SCN^- and $Si_{12}C_{12}$ in order are about 3.01 and 3.22 eV (Table 1). This amount of E_g for the $Si_{12}C_{12}$ substrate indicates semiconductor features [40]. Fig. 2 shows that the HOMO orbital for the most stable compound (model I) is slightly situated around the S–C–N bond and is evenly distributed on the C atoms of $Si_{12}C_{12}$ at an energy level of −2.92 eV. The LUMO orbital of model I is uniformly situated throughout the Si—C bonds of the $Si_{12}C_{12}$ at an energy level of 0.12 eV. In contrast, the HOMO (alpha) orbital for two SCN^- molecules adsorbed on the Si—Si atoms of $Si_{12}C_{12}$ substrate is

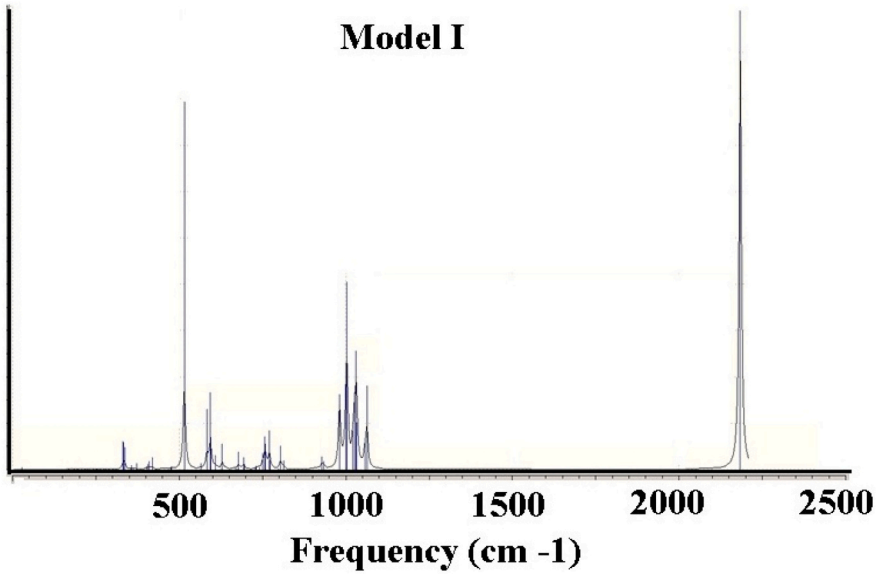

Fig. 5. IR spectrum of $SCN^{-}/Si_{12}C_{12}$ complex.

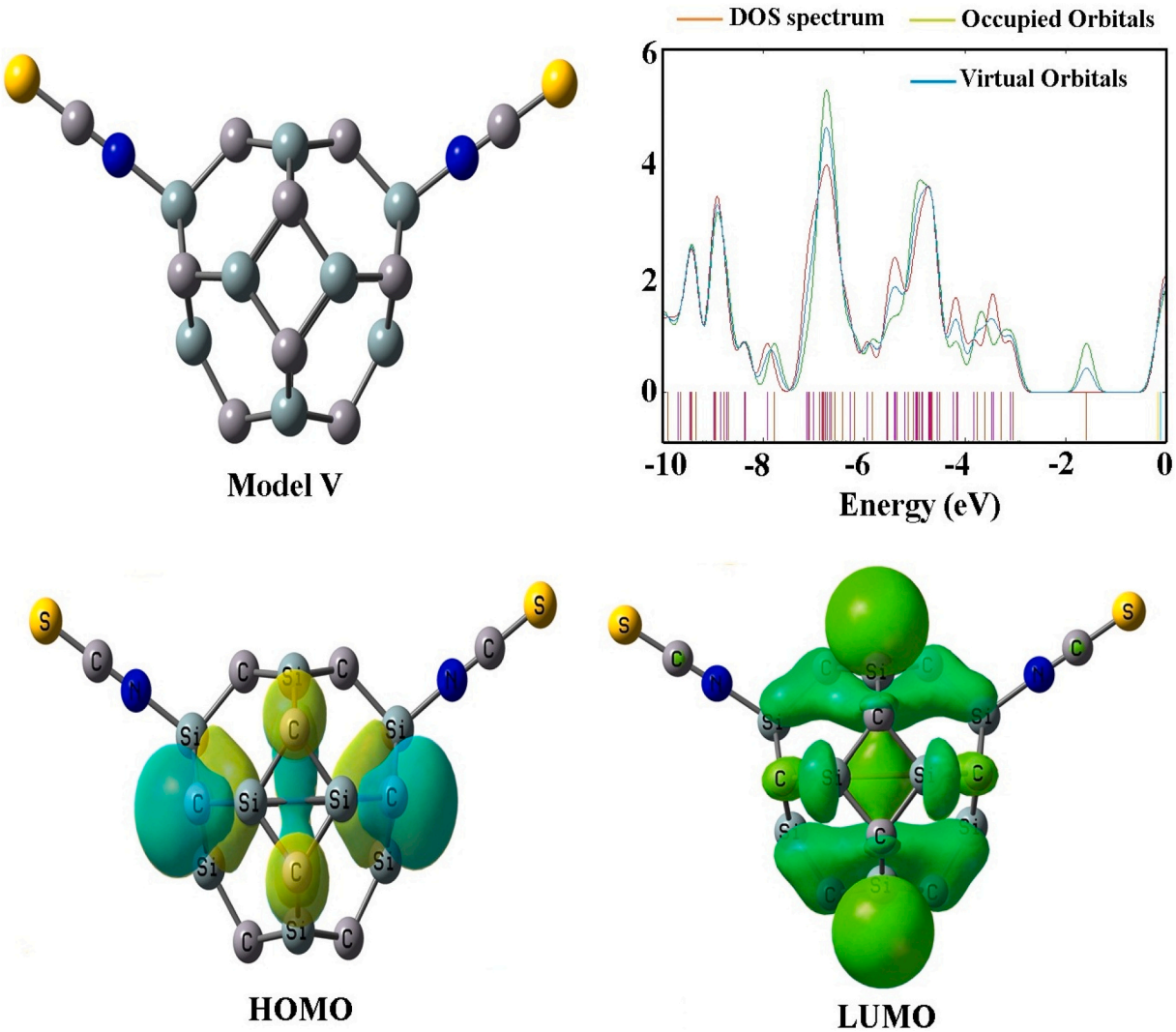

Fig. 6. The FMO and DOS plots for the two $SCN^{-}/Si_{12}C_{12}$ (V) complexes.

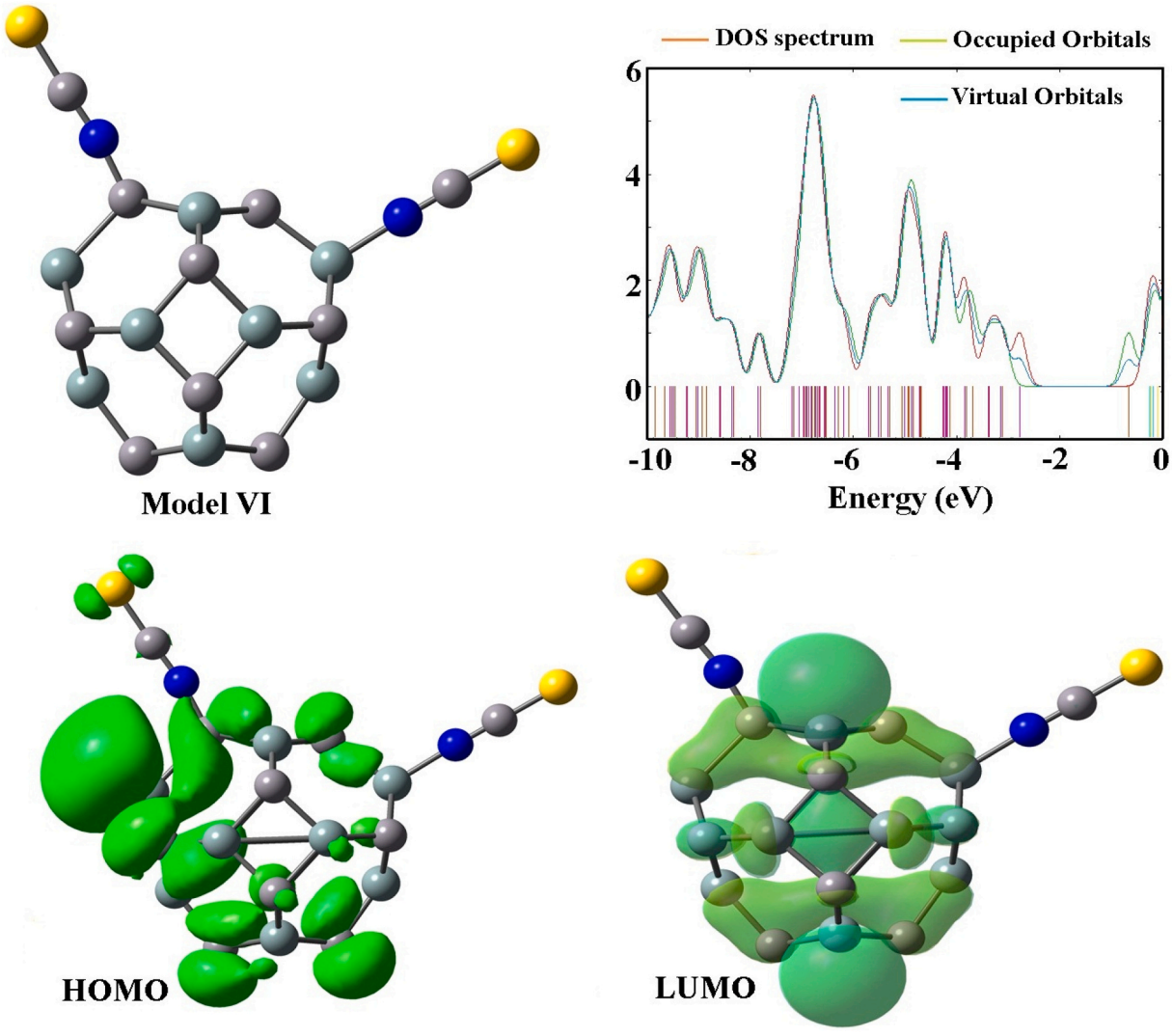

Fig. 7. The FMO and DOS plots for the two $SCN^-/Si_{12}C_{12}$ (VI) complexes.

Table 1
Calculated HOMO energies (E_{HOMO}/eV), LUMO energies (E_{LUMO}/eV), dipole moment (μ_D/Debye), and energy gap (E_g/eV) for the pure and their complexes.

Property	SCN^-	$Si_{12}C_{12}$	N-side (I)	N-side (II)	S-side (III)	S-side (IV)	N-side (V)	N-side (VI)
E_{HOMO}/eV	−1.09	−6.13	−2.92	−2.01	−3.03	−3.0	−3.09	−2.78
E_{LUMO}/eV	4.10	−2.91	0.12	−0.30	0.04	0.04	−0.13	−0.26
E_g/eV	3.10	3.22	3.04	1.71	3.07	3.04	2.96	2.52
μ_D/Debye	0.67	0.0	18.87	20.81	17.63	18.56	17.10	20.68
E_F/eV	–	−4.52	−1.40	−1.16	−1.50	−1.48	−1.61	−1.52
ΔE_g/%	–	–	5.59	46.89	4.66	5.59	8.07	21.74

evenly distributed on the C atoms of $Si_{12}C_{12}$ at an energy level of −3.09 eV, while the LUMO orbital is evenly distributed on the Si—C bonds of $Si_{12}C_{12}$ and slightly situated on the carbon atoms of two SCN^- molecules at an energy level of −0.13 eV (Figs. 6–7). The DOS of the $Si_{12}C_{12}$ substrate was compared with those of the $SCN^-/Si_{12}C_{12}$ and $2SCN^-/Si_{12}C_{12}$ complexes in order to examine the binding effect on the electronic features of these complexes (Figs. 2, 4, 6, 7). According to DOS analysis, the E_g value of SCN^- through N-side (3.04 eV) and S-side (3.07 eV) interacting with $Si_{12}C_{12}$ is slightly altered when compared with two SCN^- through N-side interacting with $Si_{12}C_{12}$ substrate (2.96 eV). These findings suggest that the SCN^- interacting with the silicon atom of $Si_{12}C_{12}$ does not significantly affect the electronic properties of the substrate, while the adsorption of SCN^- on the carbon atom of $Si_{12}C_{12}$ could improve the sensitivity of the substrate to the molecule [41]. Furthermore, the Fermi level (E_F) results show a value of −4.52 eV in order for the pure $Si_{12}C_{12}$ to −1.40 eV and −1.50 eV for SCN^- through N-side and S-side positions on the $Si_{12}C_{12}$ substrate, extract the strong charge transfer as probable. For two SCN^- molecules interacting with the $Si_{12}C_{12}$ substrate, the value of E_F is changed to −1.61 eV. After the adsorption process, the energy gap change (ΔE_g) in model II (46.89 %) is reduced than in model I (5.59 %). Therefore, unlike silicon atoms in $Si_{12}C_{12}$, carbon atoms in $Si_{12}C_{12}$ can efficiently sense SCN^-. The results of ΔE_g suggest that the role of carbon atoms in the substrate for the detection of one or two SCN^- molecules (model VI) (Fig. 9). Iman and co-authors experimentally showed the role of Co_7 clusters in the detection of thiocyanate anions by spectroscopic and DFT methods [42].

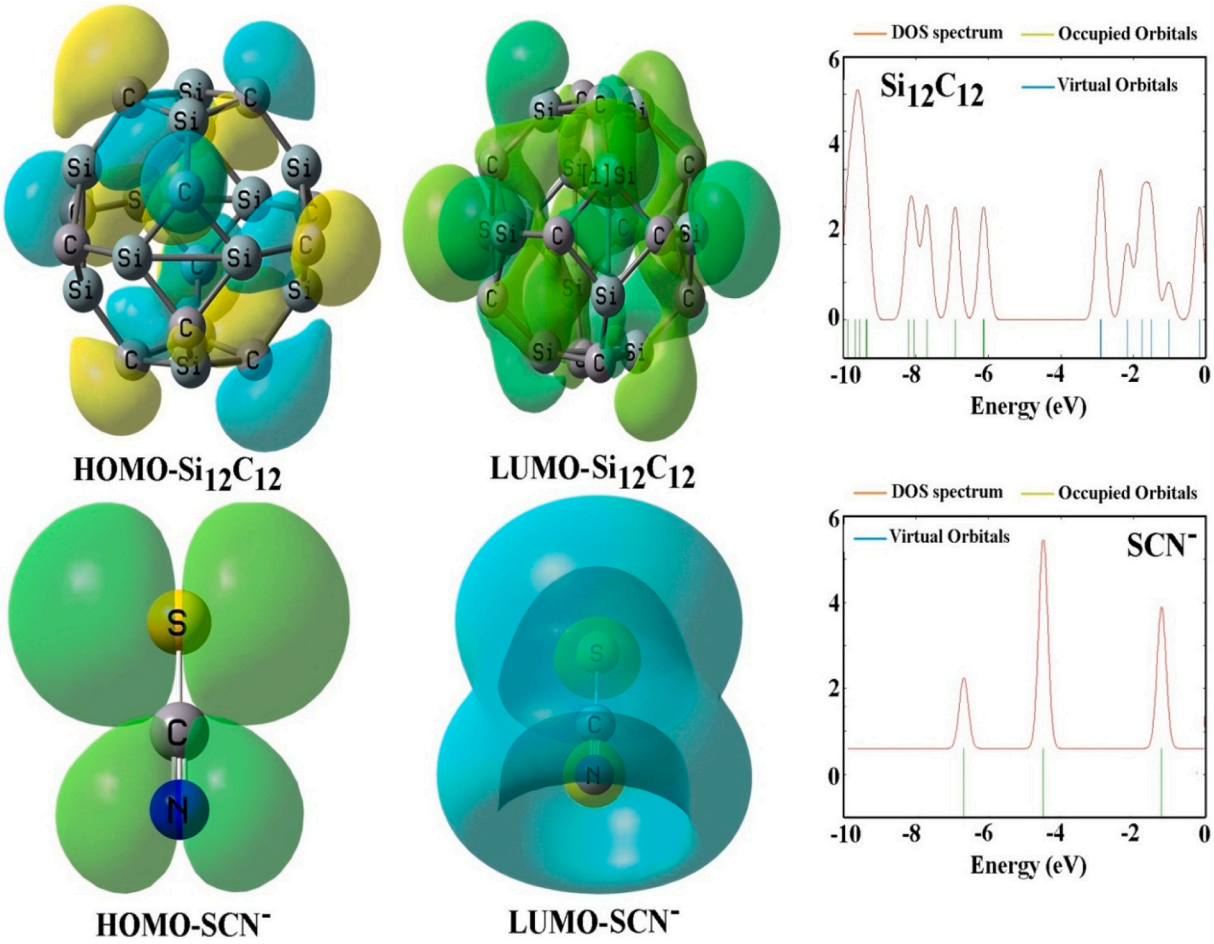

Fig. 8. The FMO plot for the SCN^- and $Si_{12}C_{12}$ compounds.

They found that the Co_7 cluster has a better quenching ability toward the recognition of SCN^- with a better binding constant. Reducing E_g increases the complex electrical conductivity that can be converted into an electrical signal for SCN^- detection by the $Si_{12}C_{12}$ substrate [43]. Therefore, SiC fullerenes can be used to filter out hazardous molecules and gas-sensing fields [44].

3.3. QMD for $SCN^-/Si_{12}C_{12}$ complexes

The QMD results demonstrate a reduction in energy gap, which causes the decrement in *I* from 6.13 eV for pure $Si_{12}C_{12}$ to 2.92 and 2.01 eV for SCN^- via its N-side close to a silicon atom of the $Si_{12}C_{12}$ fullerene, while the A value with the SCN^- adsorption through N-side on the silicon atom of the $Si_{12}C_{12}$ will lead to a reduction from 2.91 eV to 0.12 and 0.30 eV in models I and II, respectively (Table 2). The lowest electronegativity (χ) is calculated for model II (1.16 eV) in comparison with the pure substrate (4.52 eV). The μ value for SCN^- via its N-side approaching silicon (model I) and carbon (model II) atoms of the $Si_{12}C_{12}$ substrate is reduced from −4.52 eV in the perfect substrate to −1.52 and −1.16 eV for $SCN^-/Si_{12}C_{12}$ complexes, respectively. Based on the chemical potential (μ) analysis, model II has the lowest μ value, thus, this complex has less reactivity [45]. The lowest η value was obtained for models I (1.40 eV) and model II (0.86 eV) compared to models III (150 eV) and IV (1.48 eV), while the amount of η for the pure substrate is found to be 1.61 eV. This decrement in η value for the complexes is resulting from low electron affinity and ionization potential and leads to its higher reactivity [46]. The highest softness (S) is calculated for model I (0.36 eV) and II (0.58 eV) in comparison with the pure substrate (0.31 eV). Adsorption of SCN^- via its N-side approaching carbon (model II) atom of the $Si_{12}C_{12}$ substrate is increased in comparison with the SCN^- via its N-side approaching silicon (model I) atom of the $Si_{12}C_{12}$ substrate. Electrophilicity index (ω) for the SCN^- through N-side interacting with $Si_{12}C_{12}$ has a noticeable reduction from 6.34 eV in the perfect substrate to 0.825 eV (I) and 0.780 eV (II) compared to the SCN^- adsorption through N-side in model III (0.788 eV) and model IV (0.780 eV).

4. Conclusion

DFT calculations were used for the SCN^- adsorption ability on the perfect $Si_{12}C_{12}$ fullerene at the B3LYP/6-31G** level of theory to analyze the geometric, electronic properties, and adsorption behavior. Our computational study demonstrates that the adsorption properties of SCN^- through nitrogen head (−3.08 eV) on the $Si_{12}C_{12}$ fullerene is most notable when compared to the SCN^- adsorption through sulfur head (−2.32 eV). Additionally, the interaction of two SCN^- through nitrogen head has weaker surface adsorption on the Si—C atom (−1.27 eV) in comparison with the Si—Si atom (−2.78 eV) of $Si_{12}C_{12}$ fullerene. Based on our findings, it seems that silicon atom affection on the interaction of SCN^- molecule with the $Si_{12}C_{12}$ fullerene as lead to the improvement of adsorption energy. In contrast, the carbon atoms of the $Si_{12}C_{12}$ have a significant role in the alteration of the electrical conductance and dipole moment of the substrate. A significant orbital hybridization between SCN^- and $Si_{12}C_{12}$ fullerenes occurred during the adsorption process, according to the computed density of states (DOS). Hence, the SCN^- adsorption$^-$ on the carbon atom of $Si_{12}C_{12}$ (model II) lead to the reduction in E_g values, ionization potential, chemical hardness, electronegativity, and electrophilicity index. According to the

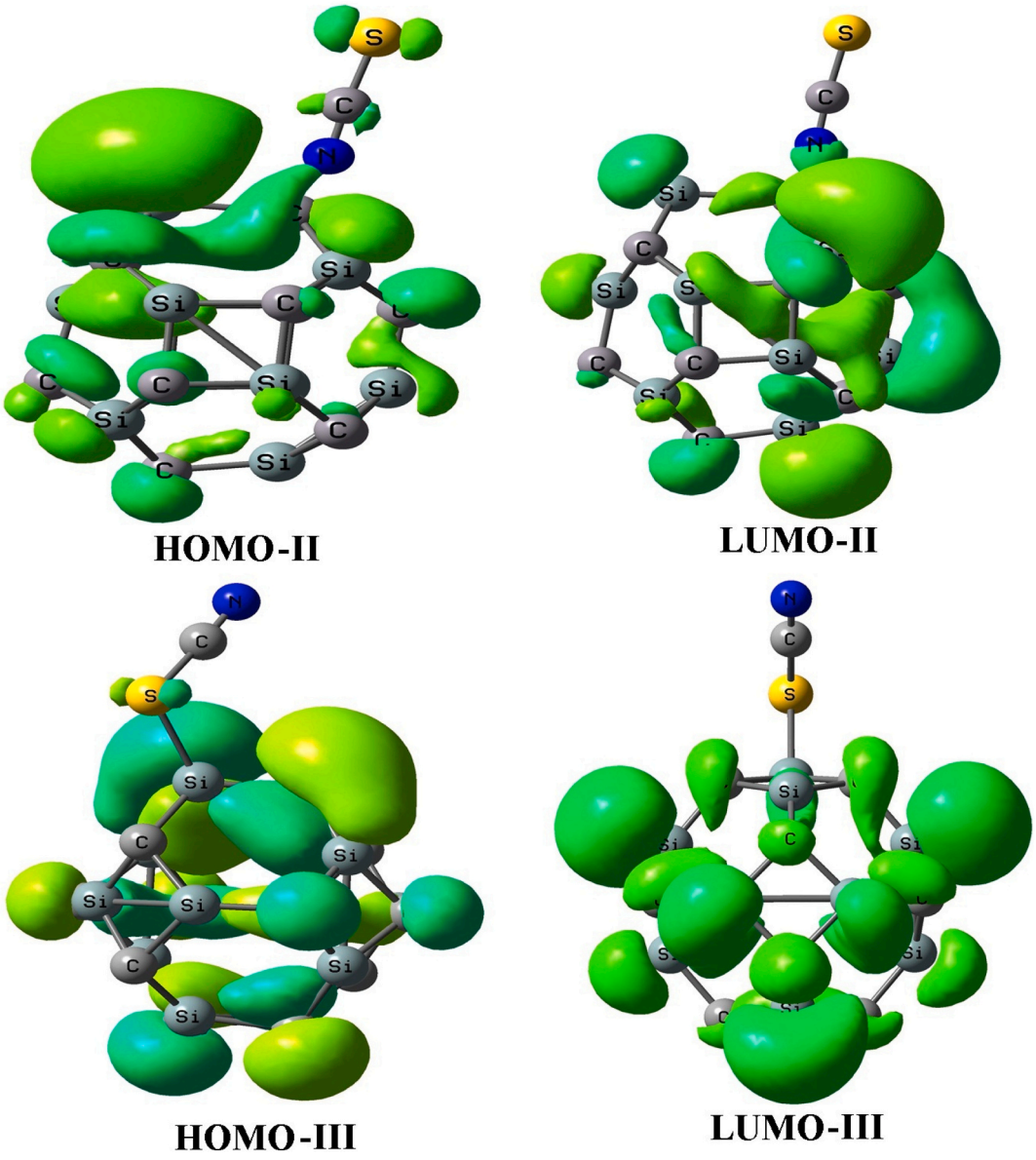

Fig. 9. HOMO and LUMO plots for the SCN^- interacting with $Si_{12}C_{12}$ fullerene.

Table 2
Calculated QMD values for the pure and their complexes.

Property	SCN^-	$Si_{12}C_{12}$	N-side (I)	N-side (II)	S-side (III)	S-side (IV)	N-side (V)	N-side (VI)
I/eV	1.09	6.13	2.92	2.01	3.03	3.0	3.09	2.78
A/eV	−4.10	2.91	0.12	0.30	0.04	0.04	0.13	0.26
η/eV	2.59	1.61	1.40	0.86	1.50	1.48	1.48	1.26
μ/eV	1.51	−4.52	−1.52	−1.16	−1.54	−1.52	−1.61	−1.52
S/eV	0.19	0.31	0.36	0.58	0.33	0.34	0.33	0.40
ω/eV	0.44	6.34	0.825	0.780	0.788	0.780	0.876	0.916
χ/eV	−1.51	4.52	1.52	1.16	1.54	1.52	−1.61	1.52

thermodynamic parameters, the negative ΔG and ΔH values confirmed that the SCN^- adsorption by the nitrogen heads on $Si_{12}C_{12}$ surface was spontaneous and exothermic.

CRediT authorship contribution statement

Fangyuan Li: Supervision, Writing – review & editing. **Fay Fathdal:** Writing – review & editing, Supervision. **Gufran Abd:** Writing – review & editing, Supervision. **Jameel Mohammed Ameen Sulaiman:** Writing – review & editing. **Safaa Mustafa Hameed:** Writing – review & editing. **Sarah Salah Jalal:** Methodology, Writing – original draft. **Usama S. Altimari:** Methodology, Writing – original draft. **Israa Alhan:** Formal analysis, Software. **Ibrahim H. Alkersan:** Formal analysis, Software. **Ali H. Alsalamy:** Formal analysis, Software. **Elham Tazikeh-Lemeski:** Conceptualization, Data curation, Formal analysis, Investigation, Software. **Andrew Ng Kay Lup:** Conceptualization, Data curation, Formal analysis, Investigation, Software.

Declaration of competing interest

The authors declare that they have no known competing financial interests or personal relationships that could have appeared to influence the work reported in this paper.

Data availability

No data was used for the research described in the article.

Acknowledgment

We thank Zhejiang Business Technology Institute and Xiamen University Malaysia for their valuable contributions to this research.

References

[1] J. Prakash, R. Venugopalan, B.M. Tripathi, S.K. Ghosh, J.K. Chakravartty, A. K. Tyagi, Chemistry of one dimensional silicon carbide materials: principle, production, application and future prospects, Prog. Solid State Chem. 43 (2015) 98–122.
[2] A. Oliveros, A. Guiseppi-Elie, S.E. Saddow, Silicon carbide: a versatile material for biosensor applications, Biomed. Microdevices 15 (2013) 353–368.
[3] P. Djemia, K. Bouamama, Ab-initio calculations of the photoelastic constants of the cubic SiC polytype, J. Phys. Conf. Ser. 454 (2013), 012060.
[4] A. Soltani, M. Ramezani Taghartapeh, V. Erfani-Moghadam, M. Bezi Javan, F. Heidari, M. Aghaei, P.J. Mahon, Serine adsorption through different functionalities on the $B_{12}N_{12}$ and Pt-$B_{12}N_{12}$ nanocages, Mater. Sci. Eng. C 92 (2018) 216–227.
[5] A. Soltani, M. Bezi Javan, M.T. Baei, Z. Azmoodeh, Adsorption of chemical warfare agents over C_{24} fullerene: effects of decoration of cobalt, J. Alloys Compd. 735 (2018) 2148–2161.
[6] A. Soltani, Z. Azmoodeh, M. Bezi Javan, E. Tazikeh Lemeski, L. Karami, A DFT study of adsorption of glycine onto the surface of BC_2N nanotube, Appl. Surf. Sci. 384 (2016) 230–236.
[7] H. Goudarziafshar, M. Abdolmaleki, A.R. Moosavi-zare, H. Soleymanabadi, Hydrogen storage by Ni-doped silicon carbide nanocage: a theoretical study, Phys. E. 101 (2018) 78–84.
[8] N. Kosar, S. Munsif, K. Ayub, T. Mahmood, Storage and permeation of hydrogen molecule, atom and ions (H+ and H-) through silicon carbide nanotube; a DFT approach, Int. J. Hydrog. Energy 46 (2021) 9163–9173.
[9] M. Solimannejad, A. Karimi Anjiraki, S. Kamalinahad, Sensing performance of Cu-decorated $Si_{12}C_{12}$ nanocage towards toxic cyanogen gas: a DFT study, Mater. Res. Express 4 (2017), 045011.
[10] M. Bezi Javan, Adsorption of CO and NO molecules on SiC nanotubes and nanocages: DFT study, Surf. Sci. 635 (2015) 128–142.
[11] S.M. Alshahrani, S. Alshehri, A.M. Alsubaiyel, R.M. Alzhrani, A.D. Alatawi, M. A. Algarni, M.H. Abduljabbar, A. Ng Kay Lup, M.S. Sarjad, M.L. Rahman, M.A. S. Abourehab, A robust computational investigation on C_{60} fullerene nanostructure as a novel sensor to detect SCN^-, Arab. J. Chem. 15 (2022), 104336.
[12] M.T. Baei, A.S. Ghasemi, E. Tazikeh-Lemeski, A. Soltani, F. Ashrafi, S. Sedighi, Effect of adsorption sensitivity of armchair single-walled BN nanotube toward thiocyanate anion: a systematic evaluation of length and diameter effects, Surf. Interfaces 21 (2020), 100693.
[13] A. Soltani, M.R. Taghartapeh, H. Mighani, A.A. Pahlevani, R. Mashkoor, A first-principles study of the SCN- chemisorption on the surface of AlN, AlP, and BP nanotubes, Appl. Surf. Sci. 259 (2012) 637–642.
[14] A. Soltani, N. Ahmadian, Y. Kanani, A. Dehnokhalaji, H. Mighani, Ab initio investigation of the SCN^- chemisorption of singlewalled boron nitride nanotubes, Appl. Surf. Sci. 258 (2012) 9536–9543.
[15] A. Soltani, M.T. Baei, E. Tazikeh Lemeski, A.A. Pahlevani, The study of SCN^- adsorption on $B_{12}N_{12}$ and $B_{16}N_{16}$ nano-cages, Superlattice. Microst. 75 (2014) 716–724.
[16] R. Rahimi, M. Solimannejad, Hydrazine trapping ability of $Si_{12}C_{12}$ fullerene-like nanoclusters: a DFT study, Struct. Chem. 31 (2020) 133–140.
[17] M.J. Frisch, G.W. Trucks, H.B. Schlegel, G.E. Scuseria, M.A. Robb, J.R. Cheeseman, J.A. Montgomery Jr., T. Vreven, K.N. Kudin, J.C. Burant, J.M. Millam, S.S. Iyengar, J. Tomasi, V. Barone, B. Mennucci, M. Cossi, G. Scalmani, N. Rega, G.A. Petersson, H. Nakatsuji, M. Hada, M. Ehara, K. Toyota, R. Fukuda, J. Hasegawa, M. Ishida, T. Nakajima, Y. Honda, O. Kitao, H. Nakai, M. Klene, X. Li, J.E. Knox, H. P. Hratchian, J.B. Cross, V. Bakken, C. Adamo, J. Jaramillo, R. Gomperts, R. E. Stratmann, O. Yazyev, A.J. Austin, R. Cammi, C. Pomelli, J.W. Ochterski, P. Y. Ayala, K. Morokuma, G.A. Voth, P. Salvador, J.J. Dannenberg, V.G. Zakrzewski, S. Dapprich, A.D. Daniels, M.C. Strain, O. Farkas, D.K. Malick, A.D. Rabuck, K. Raghavachari, J.B. Foresman, J.V. Ortiz, Q. Cui, A.G. Baboul, S. Clifford, J. Cioslowski, B.B. Stefanov, G. Liu, A. Liashenko, P. Piskorz, I. Komaromi, R. L. Martin, D.J. Fox, T. Keith, M.A. AlLaham, C.Y. Peng, A. Nanayakkara, M. Challacombe, P.M.W. Gill, B. Johnson, W. Chen, M.W. Wong, C. Gonzalez, J. A. Pople, Gaussian 09, Revision A01, Gaussian, Inc., Wallingford, CT, 2009.
[18] N.M. O'Boyle, A.L. Tenderholt, K.M. Langner, cclib: a library for package-independent computational chemistry algorithms, J. Comput. Chem. 29 (2008) 839–845.
[19] R.D. Dennington, T.A. Keith, J.M. Millam, GaussView 5.0.8, Gaussian, 2008.
[20] A.D. Becke, Density-functional thermochemistry. III. The role of exact exchange, J. Chem. Phys. 98 (1993) 5648.
[21] C. Lee, W. Yang, R.G. Parr, Development of the Colle-Salvetti correlation-energy formula into a functional of the electron density, Phys. Rev. B 37 (1988) 785.
[22] R.G. Parr, W. Yang, Density Functional Theory of Atoms and Molecules, Oxford University Press, NewYork, 1989.
[23] A. Soltani, F. Ghari, A. Dehno Khalaji, E. Tazikeh Lemeski, K. Fejfarova, M. Dusek, M. Shikhi, Crystal structure, spectroscopic and theoretical studies on two Schiff base compounds of 2,6-dichlorobenzylidene-2,4-dichloroaniline and 2,4-dichlorobenzylidene-2,4-dichloroaniline, Spectrochim. Acta A Mol. Biomol. Spectrosc. 139 (2015) 271–278.
[24] M.T. Baei, Y. Kanani, V. Joveini Rezaei, A. Soltani, Adsorption phenomena of gas molecules upon Ga-doped BN nanotubes: a DFT study, Appl. Surf. Sci. 295 (2014) 18–25.
[25] M. Solimannejad, A. Karimi Anjiraki, S. Kamalinahad, Sensing performance of Cu-decorated $Si_{12}C_{12}$ nanocage towards toxic cyanogen gas: a DFT study, Mater. Res. Express 4 (2017), 045011.
[26] Y. Li, C. Chen, J.-T. Li, Y. Yang, Z.-M. Lin, Surface charges and optical characteristic of colloidal cubic SiC nanocrystals, Nanoscale Res. Lett. 6 (2011) 454.
[27] A. Dehno Khalaji, M. Weil, H. Hadadzadeh, M. Daryanavard, Two different 1D-chains in the structures of the copper(I) coordination polymers based on bidentate Schiff-base building units and thiocyanate anions as bridging ligands, Inorg. Chim. Acta 362 (2009) 4837.
[28] T. Lu, F. Chen, Multiwfn: a multifunctional wavefunction analyzer, J. Comput. Chem. 33 (2012) 580–592.
[29] K. Hachem, M. Jade Catalan Opulencia, W. Kamal Abdelbasset, A. Sevbitov, O. R. Kuzichkin, A. Mohamed, S. Moazen Rad, A. Salehi, J. Kaur, R. Kumar, A. Ng Kay Lup, A. Arian Nia, Anti-inflammatory effect of functionalized sulfasalazine boron nitride nanocages on cardiovascular disease and breast cancer: an in-silico simulation, J. Mol. Liq. 356 (2022), 119030.
[30] A. Soltani, N. Ahmadian, Y. Kanani, A. Dehnokhalaji, H. Mighani, Ab initio investigation of the SCN^- chemisorption of single-walled boron nitride nanotubes, Appl. Surf. Sci. 258 (2012) 9536–9543.
[31] K. Iman, M. Naqi Ahamad, Monika, A. Ansari, H.A.M. Saleh, M. Shahnawaz Khan, M. Ahmad, R.A. Haque, M. Shahid, How to identify a smoker: a salient crystallographic approach to detect thiocyanate content, RSC Adv. 11 (2021) 16881.
[32] I. Karbovnyk, P. Savchyn, A. Huczko, M. Cestelli Guidi, C. Mirri, A.I. Popov, FTIR studies of silicon carbide 1D-nanostructures, Mater. Sci. Forum 821–823 (2015) 261–264.
[33] K. Derakhshan Karjabad, S. Mohajeri, A. Shamel, M. Khodadadi-Moghaddam, G. Ebrahimzadeh Rajaei, Boron nitride nanoclusters as a sensor for Cyclosarin nerve agent: DFT and thermodynamics studies, SN Appl. Sci. 2 (2020) 574.
[34] A. Soltani, M. Bezi Javan, M.S. Hoseininezhad-Namin, N. Tajabor, E. Tazikeh Lemeski, F. Pourarian, Interaction of hydrogen with Pd- and co-decorated C24 fullerenes: density functional theory study, Synth. Met. 234 (2017) 1–8.
[35] E. Tazikeh-Lemeski, A. Soltani, M.T. Baei, M. Bezi Javan, S. Moazen Rad, Theoretical study on pure and doped B12N12 fullerenes as thiophene sensor, Adsorption 24 (2018) 585–593.
[36] A.S. Ghasemi, M. Ramezani Taghartapeh, A. Soltani, P.J. Mahon, Adsorption behavior of metformin drug on boron nitride fullerenes: thermodynamics and DFT studies, J. Mol. Liq. 275 (2019) 955–967.
[37] F. Ullaha, N. Kosara, M. Nadeem Arshad, M.A. Gilanid, K. Ayuba, T. Mahmood, Design of novel superalkali doped silicon carbide nanocages with giant nonlinear optical response, Opt. Laser Technol. 122 (2020), 105855.
[38] S.S. Dindorkar, A. Yadav, Monolayered silicon carbide for sensing toxic gases: a comprehensive study based on the first-principle density functional theory, Silicon 14 (2022) 11771–11779.
[39] K. Iman, M. Naqi Ahamad, Monika, A. Ansari, H.A.M. Saleh, M. Shahnawaz Khan, M. Ahmad, R.A. Haque, M. Shahid, How to identify a smoker: a salient crystallographic approach to detect thiocyanate content, RSC Adv. 11 (2021) 16881–16891.
[40] L. Sun, Han, N. Wu, B. Wang, Y. Wang, High temperature gas sensing performances of silicon carbide nanosheets with an n–p conductivity transition, RSC Adv. 8 (2018) 13697.
[41] X. Zhang, D. Shao, W. Lyu, G. Tan, H. Ren, Utilizing discarded SiC heating rod to fabricate SiC/Sb-SnO_2 anode for electrochemical oxidation of wastewater, Chem. Eng. J. 361 (2019) 862–873.
[42] A. Soltani, E. Tazikeh-Lemeski, M.B. Javan, A comparative theoretical study on the interaction of pure and carbon atom substituted boron nitride fullerenes with ifosfamide drug, J. Mol. Liq. 297 (2020), 111894.
[43] H. Farrokhpour, H. Jouypazadeh, S. Vakili Sohroforouzani, Interaction of different types of nanocages ($Al_{12}N_{12}$, $Al_{12}P_{12}$, $B_{12}N_{12}$, $Be_{12}O_{12}$, $Mg_{12}O_{12}$, $Si_{12}C_{12}$ and C_{24}) with HCN and ClCN: DFT, TD-DFT, QTAIM, and NBO calculations, Mol. Phys. 118 (2020) 1–12.
[44] M.S. Hoseininezhad-Namin, P. Pargolghasemi, M. Saadi, M. Ramezani Taghartapeh, N. Abdolahi, A. Soltani, A.N.K. Lup, Ab initio study of TEPA

adsorption on pristine, Al and Si doped carbon and boron nitride nanotubes, J. Inorg. Organomet. Polym. 30 (2020) 4297–4310.

[45] A. Soltani, A. Khan, H. Mirzaei, M. Onaq, M. Javan, S. Tavassoli, N.O. Mahmoodi, A. Arian Nia, A. Yahyazadeh, A. Salehi, S.R. Khandoozi, R.K. Masjedi, M. L. Rahman, M.S. Sarjadi, S.M. Sarkar, C.-H. Su, Improvement of anti-inflammatory and anticancer activities of poly(lactic-co-glycolic acid)-sulfasalazine microparticle via density functional theory, molecular docking and ADMET analysis, Arab. J. Chem. 15 (2022), 103464.

[46] Y. Cao, M. Noori, M. Nazari, A. Ng Kay Lup, A. Soltani, V. Erfani-Moghadam, A. Salehi, M. Aghaei, M.L. Rahman, M. Sani Sarjadi, S.M. Sarkar, C.-H. Su, Molecular docking evaluation of celecoxib on the boron nitride nanostructures for alleviation of cardiovascular risk and inflammatory, Arab. J. Chem. 15 (2022), 103521.